BJR
© 2015 The Authors. Published by the British Institute of Radiology

Received: 11 March 2015 | Revised: 8 May 2015 | Accepted: 12 May 2015

doi: 10.1259/bjr.20150207

Cite this article as:
Baetke SC, Lammers T, Kiessling F. Applications of nanoparticles for diagnosis and therapy of cancer. *Br J Radiol* 2015; **88**: 20150207.

NANOPARTICLES FOR DIAGNOSTIC IMAGING AND RADIOTHERAPY SPECIAL FEATURE: REVIEW ARTICLE

Applications of nanoparticles for diagnosis and therapy of cancer

S C BAETKE, MSc, T LAMMERS, PhD, DSc and F KIESSLING, MD

Department of Experimental Molecular Imaging, Helmholtz Institute for Biomedical Engineering, RWTH Aachen University, Aachen, Germany

Address correspondence to: Professor Fabian Kiessling
E-mail: *fkiessling@ukaachen.de*

ABSTRACT

During the last decades, a plethora of nanoparticles have been developed and evaluated and a real hype has been created around their potential application as diagnostic and therapeutic agents. Despite their suggestion as potential diagnostic agents, only a single diagnostic nanoparticle formulation, namely iron oxide nanoparticles, has found its way into clinical routine so far. This fact is primarily due to difficulties in achieving appropriate pharmacokinetic properties and a reproducible synthesis of monodispersed nanoparticles. Furthermore, concerns exist about their biodegradation, elimination and toxicity. The majority of nanoparticle formulations that are currently routinely used in the clinic are used for therapeutic purposes. These therapeutic nanoparticles aim to more efficiently deliver a (chemo-) therapeutic drug to the pathological site, while avoiding its accumulation in healthy organs and tissues, and are predominantly based on the "enhanced permeability and retention" (EPR) effect. Furthermore, based on their ability to integrate diagnostic and therapeutic entities within a single nanoparticle formulation, nanoparticles hold great promise for theranostic purposes and are considered to be highly useful for personalizing nanomedicine-based treatments. In this review article, we present applications of diagnostic and therapeutic nanoparticles, summarize frequently used non-invasive imaging techniques and describe the role of EPR in the accumulation of nanotheranostic formulations. In this context, the clinical potential of nanotheranostics and image-guided drug delivery for individualized and improved (chemo-) therapeutic interventions is addressed.

Currently, *in vivo* molecular imaging comprises an important focus area of medical research. The rapidly evolving field of molecular imaging improves early disease detection and disease staging and enables image-guided therapy and treatment personalization. Furthermore, it provides essential information on the therapy efficacy. However, molecular imaging requires the use of molecular imaging probes to visualize and characterize biological processes at the cellular and molecular level.[1–5]

Recent advances in nanotechnology have led to the development of various nanoparticle formulations for diagnostic and therapeutic applications. Diagnostic nanoparticles aim to visualize pathologies and to improve the understanding of important (patho-) physiological principles of various diseases and disease treatments. Clinically, however, nanodiagnostics are only useful in a limited number of situations, due to the complex demands on their pharmacokinetic properties and elimination. Therefore, the majority of nanoparticle formulations currently used in the clinics is applied for therapeutic purposes. Therapeutic nanoparticles aim to improve the accumulation and release of pharmacologically active agents at the pathological site, increase therapeutic efficacy and reduce the incidence and intensity of side effects by reducing their localization in healthy tissues.[6–9] The intrinsic characteristics of nanoparticles hold great promise for integrating diagnostic and therapeutic agents into a single nanoparticle formulation, enabling their application for theranostic purposes, such as monitoring the biodistribution and target site accumulation, visualizing and quantifying drug release and longitudinally assessing the therapeutic efficacy. Such theranostic nanoparticles may be used for personalizing nanomedicine-based therapies by enabling patient preselection and by controlling therapeutic efficacy.[7–15]

In this review article, indications of current nanoparticle formulations for diagnostic and therapeutic applications and a brief overview of non-invasive imaging modalities will be given. In addition, the suitability of nanoparticles as

molecular imaging probes and contrast agents to enhance disease diagnosis and treatment and their potential clinical application to facilitate personalized therapy interventions will be addressed and discussed.

GENERAL CONSIDERATIONS ON MEDICAL IMAGING MODALITIES AND PROBES

In this section, a brief overview of frequently used non-invasive imaging modalities with respect to the application of nanoparticles will be provided. Medical imaging comprises the non-invasive assessment of anatomical (or morphological), functional and molecular information, which enables the diagnosis of pathophysiological abnormalities. Current imaging modalities that are routinely used in preclinical research and clinical practice include MRI, CT, ultrasound, optical imaging (OI) and photoacoustic imaging (PAI), as well as positron emission tomography (PET) and single photon emission CT (SPECT). These modalities are based on different underlying physical principles and, therefore, possess specific advantages and disadvantages with respect to sensitivity and specificity to contrast agents, tissue contrast, spatial resolution, quantitativeness and tissue penetration.[3,16–18] An overview of the clinically most relevant imaging modalities and their characteristics is provided in Table 1.

The choice of an imaging method should not only be based on the type of available contrast agent but also on the intended application. For example, if whole body scans are required, modalities such as MRI, CT, PET and SPECT are recommended. However, fast and low-cost organ-specific examinations can excellently be performed by ultrasound. Optical and photoacoustic applications, however, are most suitable for investigating superficial lesions (*e.g.* skin, peripheral joints), endoscopic and intraoperative procedures.

Nanoparticles as contrast agents for functional and molecular imaging include among others polymers, liposomes, ultrasmall superparamagnetic iron oxide (USPIO) nanoparticles and gold nanoparticles. However, not every nanoparticulate contrast agent is suitable for clinical translation. One reason is that many clinical questions can already be answered without (nanoparticle) contrast agents, such as angiography by arterial spin labeling MRI. However, arterial spin labeling is not suitable for all types of tumours depending on their blood flow and the achieved signal-to-noise ratio. Alternatively, since scan times in MRI and CT have become very short, clinically approved small-molecular-weight agents can be used,[6] which reduce the need for blood pool contrast agents. For example, CT angiography was shown to reliably detect pulmonary embolism, as well as vascular damage after upper extremity trauma and the integrity of aortic stent grafts.[47] Furthermore, using clinically approved small gadolinium chelates, successful contrast-enhanced MR angiography of the coronary vasculature, the detection of atherosclerotic plaques, as well as peripheral arterial diseases has been demonstrated.[48]

For molecular imaging purposes, 5- to 100-nm sized diagnostic nanoparticle formulations are often inferior to very small (<5 nm) as well as very large (>1 μm) diagnostic agents in acquiring highly specific imaging information. The diagnostic demands on nanoparticles rely on a rapid and highly site-specific contrast enhancement. However, blood half-lives of larger diagnostic nanoparticle formulations may be too long (there will be no renal clearance for particles with sizes over 5 nm) and there may be too much unspecific retention in the extravascular compartment or too high uptake by the reticuloendothelial system (RES), all of those factors contributing to high background signal.[6] Since molecularly targeted diagnostic agents should possess high selectivity to their target, low-molecular-weight contrast agents, for which the unbound fraction is rapidly eliminated by renal clearance, tend to be optimal. Alternatively, very large imaging agents, which do not extravasate at all (and thus do not non-specifically accumulate in the extravascular space) and possess very short circulation times, are able to provide highly specific signals for intravascular targets. Consequently, diagnostic nanoparticles are often outperformed by low-molecular-weight contrast agents with respect to achieved signal-to-noise levels, pharmacokinetic properties, biodistribution and tissue penetration.

Therefore, when intending to use nanodiagnostic agents, one has to carefully consider their clinical need, the added value over current (contrast-enhanced) imaging methods and their advantage over low-molecular-weight diagnostic probes. In addition, due to the usually considerably long intracorporal persistence of these probes, potential long-term toxicity effects have to be taken into account.[11,49]

NANOPARTICLES AND THEIR PHARMACOKINETIC CHARACTERISTICS

Numerous nanoparticle formulations have been designed and evaluated over the last years, including, for example, liposomes, polymers, micelles, proteins, antibodies, gold nanoparticles, USPIO nanoparticles and nanotubes, which possess intrinsic properties that influence their biodistribution, elimination and target site accumulation (Figure 1). The majority of these nanoparticles are used for therapeutic purposes.[6,16,50,51] Currently, several therapeutic nanoparticles are applied in clinical practice. Doxil® (PEGylated, doxorubicin-loaded liposomes, Janssen Biotech, Inc., Horsham, PA), Abraxane (paclitaxel-containing albumin nanoparticles, Celgene, Summit, NJ) and AmBisome (liposomal amphotericin B, Gilead, Foster City, CA) are some prominent examples of clinically approved therapeutic nanoparticles; many other nanomedicine formulations are currently being tested in preclinical and clinical trials.[52–54] In contrast to the therapeutic application of nanoparticles, diagnostic applications are still lagging behind.[6,8] Although nanoparticles are frequently proposed as diagnostic agents, there is still only one nanoparticle formulation, namely iron oxide nanoparticles, that was used in clinical practice (ferucarbotran, Resovist; Bayer Schering Pharma, Berlin, Germany). However, even ferucarbotran was recently taken off the market. Instead, ferumoxytol (Feraheme; AMAG Pharmaceuticals Inc., Cambridge, MA), which is an FDA (Food and Drug Administration)-approved therapeutic iron oxide nanoparticle formulation for treating anaemia, is now used off-label by many radiologists.[55]

Despite enormous progress in the synthesis of novel diagnostic nanoparticle formulations, there are several limiting factors that

Table 1. Overview of routinely used imaging modalities in the clinic, their specific advantages and disadvantages and examples of nanoparticulate contrast agents for the respective imaging method. Please note that the sensitivity and penetration depth values are based both on the literature and on our own experience and strongly depend on the method and tissue properties. Compiled using information from Kunjachan et al[16] and Ehling et al[17]

Imaging method	Advantages	Disadvantages	Sensitivity to contrast agents	Nanoparticulate contrast agents
MRI	–High spatial resolution (~10–500 μm) –Unlimited penetration depth –Excellent soft tissue contrast –Versatile options for structural, functional and metabolic tissue characterization	–Low sensitivity to contrast agents –High costs –Time-intensive	Milli- to micromolar	–Gadolinium-containing probes[19] –(Ultrasmall) superparamagnetic iron oxide nanoparticles [(U)SPIO][20] –Paramagnetic liposomes and polymers[21,22] –ParaCEST agents[23] –Hyperpolarized probes[24]
CT	High resolution (~20–200 μm) –Unlimited penetration depth –Good soft tissue contrast after injection of contrast agent –Low costs –Fast	–Insufficient soft tissue contrast without injection of contrast agents –Radiation exposure –Low sensitivity to contrast agents	Millimolar	–Iodine-based micelles and liposomes[25,26] –Barium-based nanoparticles[27] –Gold-based nanoparticles[28,29] –Bismuth nanoparticles[30]
Ultrasound	–High temporal and spatial resolution (~50–100 μm) –Rapidly operable –Real-time imaging –Low costs	–User dependence –Not appropriate for whole body imaging	Single MB detectable	–Targeted and non-targeted gas-filled microbubbles[31–33] –Nanobubbles[34] –Air-releasing polymers[35]
Optical imaging	–High sensitivity for contrast agents –Broad range of probes –Low costs	–Low penetration depth (<10 cm) –High background signal –Sensitive to artefacts	Nanomolar	–Near-infrared fluorochrome-labelled nanoparticles[36] –Quantum dots[37] –Fluorescent nanoparticle probes[38]
Photoacoustic imaging	–High sensitivity –Real-time imaging –Low costs	–Limited penetration depth (up to ~5–6 cm) –Relatively low specificity to contrast agents (signal from haemoglobin)	Milli- to nanomolar	–Gold nanoparticles, gold nanorods[39] –Carbon nanotubes[40] –Fluorescent/dye-loaded nanoparticles[41]
Positron emission tomography	–Very high sensitivity –Deep penetration depth –Quantitative	–Low spatial resolution (1–2 mm) –No anatomical information –Radiation exposure –High costs	Picomolar	–Radioactive contrast agents (*e.g.* radiolabeled gold nanoshells)[42] –Polymeric nanoparticles[43]
Single photon emission CT	–Very high sensitivity –Unlimited penetration depth –Long-circulating radionuclides	–Low spatial resolution (1–2 mm) –No anatomical information –Radioactive probes –High cost	Picomolar	–Technetium-labelled gold nanoparticles[44] –Indium-labelled liposomes[45] –Nano- and microcolloids[46]

impede the clinical translation of diagnostic nanoparticles. The major difference between nanodiagnostics and nanotherapeutics is their intended pharmacological behaviour. While nanotherapeutics should possess pharmacological activity, nanodiagnostics should not generate (patho-) physiological effects. Furthermore, nanotherapeutics should be characterized by a long blood circulation time, as their main purpose is to achieve a selective accumulation of drugs in tissues characterized by enhanced permeability and retention (EPR), such as tumours. In this regard, therapeutic nanoparticle formulations are advantageous over standard low-molecular-weight drugs, as their renal excretion is reduced, causing prolonged circulation times and decreased volume of distribution. This leads to less accumulation in healthy tissue and thus less side effects and improves the ability of drug molecules to accumulate at the pathological site, and thereby increases their therapeutic efficacy.[6,8–11] For

Figure 1. Main properties of nanoparticles influencing their biodistribution, elimination and target site accumulation.

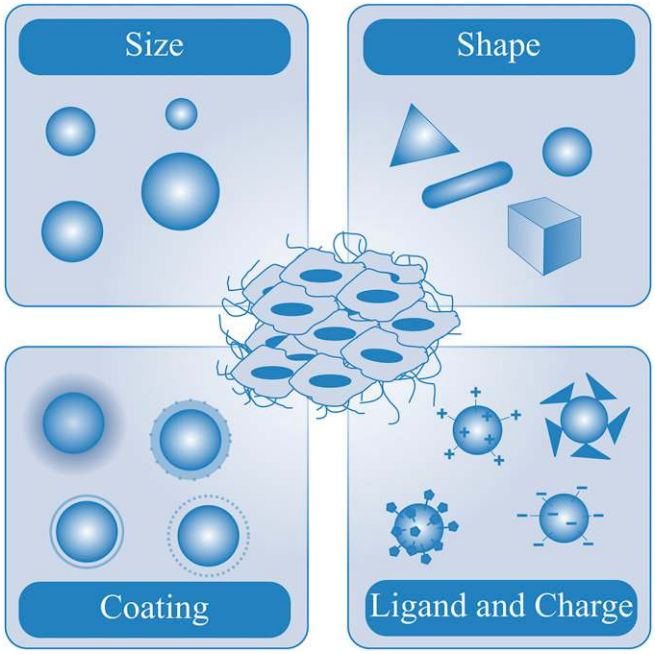

nanodiagnostics, short circulation times and fast biodegradation and elimination without pharmacological and toxicological activity are preferred. In addition, with respect to their application as molecular imaging probes, diagnostic nanoparticles should possess a good and efficient delivery to the target site and should exhibit highly specific binding and internalization capabilities. Their non-specific accumulation in healthy tissue should be low and short. Furthermore, a high sensitivity of the imaging method to detect the molecularly targeted diagnostic nanoparticles is required (ideally in the nano- to picomolar range).

Unfortunately, the intrinsic properties of nanoparticles often do not correspond with the pharmacokinetic and pharmacodynamic demands. If not taken up by the mononuclear phagocyte system (MPS) (formerly known as RES), due to their size, ranging from a few nanometres to a thousand nanometres, the biodistribution tends to be restricted to the compartment in which they were administered. For diagnostic agents targeting extravascular structures, it is essential that they rapidly extravasate out of blood vessels and penetrate and distribute within the interstitial space. The unbound fraction also has to leave these compartments rapidly in order to keep the unspecific background signal low. However, although nanoparticles accumulate in the interstitial space, their penetration into the tissue is slow and their intratumoral distribution is significantly smaller than for low-molecular-weight diagnostics.[6,8,11] It should be noted that, for therapeutic nanoparticles, it is often sufficient that the nanoparticles reach the interstitial space and here release their drug load, while tumour cell-targeted diagnostic probes need to pass the entire interstitial space to ultimately reach and bind to the tumour cell. Those demands for diagnostic nanoparticle formulations are often not adequately addressed.[6]

Nanoparticles for imaging the mononuclear phagocyte system

Most nanoparticles serve as ideal candidates to image the MPS, which comprises the liver, spleen and lymphatics. The majority of nanoparticles are taken up by the MPS due to the high content of macrophages present in those tissues. Numerous nanoparticle-based imaging agents have been proposed for diverse imaging modalities including CT, MRI, SPECT, ultrasound, OI and PAI.[39,44,56–59] However, only iron oxide nanoparticles, such as SPIOs and USPIOs, have thus far been used for clinical MPS imaging, especially for liver imaging. These nanoparticles are generally cleared from the blood *via* phagocytosis through macrophages, causing their uptake in the healthy liver, spleen and lymph nodes.[60] If it is not intended to use the nanoparticles predominantly for liver imaging but for imaging of phagocytosing cells in other tissues, for example, in lymph nodes (lymph node metastases would be positively contrasted against the healthy lymph node tissue appearing dark on T_2 weighted MR images after USPIO uptake) or in inflammatory lesions, such as atherosclerotic plaques, longer blood half-lives are required giving the particles enough time to sufficiently extravasate in the respective tissues and to be taken up by the associated macrophages. This can be reached by making the particles smaller and more monodisperse than ferucarbotran. Appealing examples have been published where (U)SPIO-enhanced MRI has been used to detect liver metastases,[61] lymph node metastases[62] and for the characterization of inflammatory lesions, such as atherosclerotic plaques.[57]

Nanoparticles for imaging tumour vascularization and angiogenesis

Imaging of tumour angiogenesis and vascularization is a reasonable indication for nanoparticulate contrast agents. While non-targeted nanoparticle formulations are applied to determine the EPR, targeted nanoparticle formulations binding to activated and proliferating endothelial cells are used to characterize tumour malignancy and aggressiveness and to assess mechanistic changes in tumour vascularization, such as vessel maturation during anti-angiogenic therapy or vascular inflammation during radiotherapy. It is not surprising that the majority of nanoparticle-based molecular imaging agents target angiogenesis since endothelial targets are most easy accessible and do not require particles' compartmental exchange. Below, several exemplary studies illustrating the application of molecular imaging methods and particulate contrast agents to assess tumour angiogenesis and anti-angiogenic therapy effects are presented.

The largest particulate molecular imaging agents are microbubbles, which are used for ultrasound imaging. In a study by Palmowski et al,[63] molecular ultrasound imaging was performed using vascular endothelial growth factor receptor 2 (VEGFR2)- and $\alpha_v\beta_3$-targeted microbubbles, demonstrating specific binding to angiogenic tumour blood vessels (Figure 2a). In addition, anti-angiogenic effects could be assessed when treating tumours with a matrix metalloproteinase inhibitor. Furthermore, molecular ultrasound imaging with the clinically translatable vascular endothelial growth factor receptor 2(VEGFR2)-targeted BR55 microbubbles (Bracco Suisse, Geneva, Switzerland) was applied to monitor anti-angiogenic treatment responses in human colon cancer xenografts[33]

Figure 2. Characterization of tumour vascularization and angiogenesis by particulate contrast agents. (a) Molecular ultrasound imaging of unconjugated, RGD-conjugated microbubbles targeted against $\alpha_v\beta_3$ integrin and VEGFR2-conjugated microbubbles, demonstrating specific binding of RGD- and VEGFR2-conjugated microbubbles to angiogenic tumour blood vessels. (b) MR molecular imaging of RGD-conjugated and RAD-modified control liposomal nanoparticles in tumour-bearing mice, showing differences in the accumulation pattern of the RGD-conjugated and RAD-modified control liposomes, which closely correlates with the position of angiogenic blood vessels in the tumour. (c) MR images of HaCaT-ras A-5RT3 tumours before and 6 h after intravenous (i.v.) injection of RGD-USPIO (ultrasmall superparamagnetic iron oxide) and USPIO nanoparticles, showing focal areas with a strong and heterogeneous decrease in signal intensity after injection of RGD-USPIO nanoparticles. (d) Fluorescence reflectance imaging of tumour accumulation of an RGD-based polymeric nanocarrier (P-RGD) and a control copolymer (P-CON) in CT26 tumours 1 and 72 h after i.v. injection, showing early binding of the actively targeted probe P-RGD to tumour blood vessels, while the passively targeted probe P-CON showed progressive enhanced permeability and retention (EPR)-mediated tumour accumulation. (e) Positron emission tomography (PET)-CT imaging of the biodistribution and tumour uptake of ^{124}I-cRGDY-PEG-C-dots in a patient with anorectal mucosal melanoma and known liver metastasis in the left hepatic lobe. (I) Coronal CT image showing a hypodense liver metastasis. (II) PET and (III) co-registered PET-CT imaging 4 h after i.v. administration of the nanoparticles demonstrate nanoparticle uptake, which appeared to be restricted to the tumour margin, as well as nanoparticle activity in the gastrointestinal tract, gallbladder, bladder and heart. (IV) PET-CT imaging 24 h after nanoparticle administration revealed clearance of the nanoparticle activity with some remaining particle activity in the tumour margin. (V) A corresponding ^{18}F-FDG PET-CT scan acquired several days after PET-CT imaging validated the localization of the liver metastasis. Adapted from Zhang et al[20], Phillips et al[54] (with permission from the American Association for the Advancement of Science), Palmowski et al[63], Mulder et al[64] (with permission from the Federation of American Societies for Experimental Biology) and Kunjachan et al[65] (with permission from the American Chemical Society).

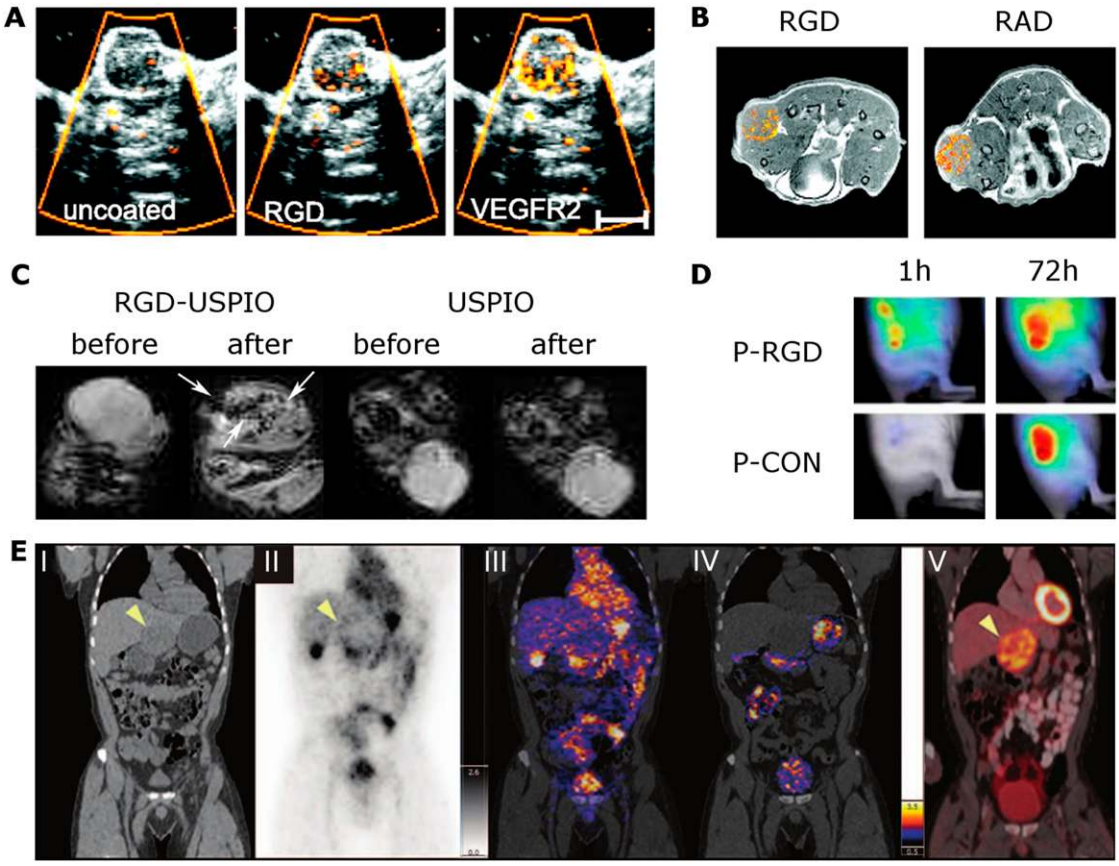

and accurately depicted the angiogenic status in two differently aggressive breast cancer xenograft models.[31] BR55 is the first lipopeptide-based microbubble formulation suited for clinical translation and is currently being evaluated in a Phase 0 clinical trial to identify patients with prostate carcinoma based on increased VEGFR2 expression in those tumours.

In another study, Mulder et al[64] used 150 nm large paramagnetic RGD-coated liposomes for molecular MRI of tumour angiogenesis and the authors demonstrated distinct differences in the tumour accumulation pattern of RGD-coated liposomes compared with non-specific RAD-coated liposomes. MRI of tumour-bearing mice injected with RGD liposomes demonstrated signal intensity increase primarily at the tumour rim 35 min after injection of the liposomes, while tumours in mice that received RAD liposomes showed signal intensity increase throughout the entire tumour (Figure 2b). In addition, a subsequent study by Mulder et al[66] was the first study showing

that anti-angiogenic therapy effects in tumours could accurately be imaged by MRI using RGD-conjugated liposomes. While the paramagnetic liposomes provided a positive MR contrast, Zhang et al[20] performed T_2 and T_2^* weighted imaging with integrin $\alpha_v\beta_3$-targeted USPIO nanoparticles that were coated with 3-aminopropyltrimethoxysilane and conjugated with cyclic RGD peptides. Imaging with these targeted probes enabled us to distinguish tumours with high and low $\alpha_v\beta_3$ integrin expression at the endothelium even when using a clinical 1.5-T MR scanner (Figure 2c).

A rather theranostic concept was evaluated by Kunjachan et al[65] who used OI to assess tumour accumulation of polymeric drug carriers conjugated with RGD- and NGR-based oligopeptides. It was shown that active targeting led to higher early accumulation of the peptide-modified probes in tumour compared with their non-targeted counterparts (Figure 2d). However, higher liver uptake of the targeted probes caused shorter blood half-lives and thus less EPR-dependent accumulation. Interestingly, since the EPR-based accumulation was contributing more to the overall accumulation than active binding, the non-targeted probes showed higher accumulation when considering the entire area under the tumour accumulation curve ($AUC_{0\text{-}72h}$). Thus, active targeting does work but does not necessarily improve nanocarrier accumulation at the target site.[65]

Recently, a first-in-human clinical trial by Phillips et al[54] demonstrated the diagnostic application of 6- to 7-nm large hybrid silica nanoparticles (C dots) in patients with metastatic melanoma (Figure 2e). The particles were labelled with ^{124}I for PET imaging and with Cy5 for OI. Specificity for $\alpha_v\beta_3$ integrins was achieved by surface functionalization with RGD peptides. The idea was that the particles enable tumour localization in the body with PET and subsequently tumour surgery under fluorescence guidance. Due to their small size, the nanoparticles are eliminated by renal clearance, instead of slower hepatic excretion. In addition, the hybrid particles were PEGylated to evade their uptake by the MPS. Multimodal imaging with the ^{124}I-cRGDY-PEG-C-dots visualized the biodistribution and tumour uptake of the nanoparticle probe in several patients. For example, PET-CT imaging 4 h after intravenous injection of the ^{124}I-cRGDY-PEG-C-dots in a patient with a liver metastasis from mucosal melanoma indicated particle uptake in the liver metastasis (Figure 2e, Panels II and III). Thus, this study demonstrates that very small nanoparticles with renal clearance have the potential to be clinically translated as multimodal diagnostic probes for cancer imaging.

Nanoparticles for imaging enhanced permeability and retention and targeted drug delivery

As already mentioned, most nanoparticle formulations were used for drug targeting to tumours and rely on the EPR effect.[67–73] Solid tumours are generally characterized by leaky blood vessels, which enable the extravasation of nanoparticles with a size of up to several hundreds of nanometres. The increased permeability of the tumour vasculature is the consequence of deregulated angiogenesis and increased release of vascular permeability enhancing factors such as VEGF. The imbalance between the formation of new blood vessels and their maturation leads to a discontinuous endothelial layer that is characterized by highly fenestrated endothelium (size of the fenestrations often >300 nm).[70] Besides the increased leakiness of tumour blood vessels, the EPR effect also depends on the fact that solid tumours lack functional lymphatic drainage, due to dysfunctional lymphangiogenesis and compression of lymphatic vessels, which limits the removal of extravasated nanoparticle formulations from the target site, leading to their prolonged retention within the pathological tissue. Below, several applications of nanoparticles for targeted drug delivery are presented.

In a study by Lammers et al,[74] poly N-(2-hydroxypropyl) methacrylamide (pHPMA)-copolymers were used as drug targeting system. The copolymers were functionalized with gadolinium and ^{131}I for imaging purposes, and with gemcitabine and doxorubicin for therapeutic purposes. The biodistribution of the copolymers was investigated by MRI and γ-scintigraphy. To more extensively evaluate tumour and organ accumulation of the polymeric drug delivery system, differently sized copolymers were radiolabeled with ^{131}I and their biodistribution was monitored by γ-scintigraphy, showing prolonged circulation and effective tumour accumulation (Figure 3a). With increasing size of the copolymers, their tumour accumulation increased (Figure 3b). Furthermore, it was shown that the HPMA-copolymers can serve as versatile and multifunctional drug carriers, which can be visualized *in vivo* after labeling with a radionuclide, and which improve the tumour-targeted delivery of low-molecular-weight drugs, resulting in enhanced antitumour efficacy.[74] In a study by Soundararajan et al,[75] ^{186}Re-labelled Doxil (PEGylated liposomal doxorubicin) was used in head and neck squamous cell carcinoma (HNSCC)-bearing nude rats and enabled the monitoring of tumour accumulation using SPECT-CT and γ-scintigraphy (Figure 3c). MicroSPECT-CT imaging (Figure 3c, left panel) and planar γ-scintigraphy (Figure 3c, right panel) 20 h after administration of ^{186}Re-Doxil proved its long blood retention, low accumulation in the liver and strong accumulation in tumours.[75] In a subsequent study by Soundararajan et al,[76] the therapeutic efficacy of ^{186}Re-labelled Doxilin combination with radiofrequency ablation therapy in HNSCC-bearing rats was assessed by tumour volume measurements and ^{18}F-FDG PET imaging, demonstrating that ^{186}Re-labelled Doxil in combination with radiofrequency ablation therapy inhibited tumour growth, increased drug accumulation in tumours and improved treatment efficiency. In another study by Koukourakis et al,[45] it was shown that radiolabeled stealth liposomal doxorubicin also enabled the visualization and quantification of EPR-mediated passive drug targeting to tumours in patients suffering from different types of sarcomas (Figure 3d). These results illustrate the capability of image-guided nanoparticles for targeted drug delivery.

TUNING THE PROPERTIES OF DIAGNOSTIC AND THERAPEUTIC NANOPARTICLES

The most important properties of nanoparticle formulations comprise particle size and charge, core and surface properties, shape and flexibility, as well as multivalency and controlled synthesis, as they determine the *in vivo* distribution, targeting ability and toxicity of the nanoparticle (Figure 1). Furthermore,

Figure 3. Theranostic applications of nanoparticles. (a) Scintigraphic analysis of the biodistribution of two differently sized ^{131}I-labelled HPMA copolymers in AT1 tumours, demonstrating effective tumour accumulation and prolonged circulation (B, bladder; H, heart; L, liver; S, spleen; T, tumour). (b) Tumour and organ concentrations of the two radiolabeled copolymers 24 and 168 h after intravenous (i.v.) administration, showing significantly higher concentrations in tumour compared with the concentrations in other healthy organs (except for the lung and spleen). (c) MicroSPECT-CT imaging (left panel) and scintigraphic analysis (right panel) of ^{186}Re-labelled Doxil® in HNSCC-bearing nude rats 20 h after i.v. administration of ^{186}Re-labelled Doxil, demonstrating prolonged blood retention and effective tumour accumulation of ^{186}Re-labelled Doxil (H, heart; L, liver; S, spleen; T, tumour). (d) Planar scintigraphic analysis of stealth liposomal doxorubicin in patients suffering from sarcomas undergoing radiotherapy reveals intense drug accumulation in tumours, demonstrating the feasibility of visualizing and quantifying EPR-mediated passive drug targeting to tumours (from left to right: fibrosarcoma of the iliac region, angiosarcoma of the maxillary antrum, Ewing sarcoma of the femur, Kaposi sarcoma of the palmar region). Adapted from Koukourakis et al[45], Lammers et al[74] and Soundararajan et al[75] with permission from Informa Healthcare, Nature Publishing Group and Elsevier, respectively.

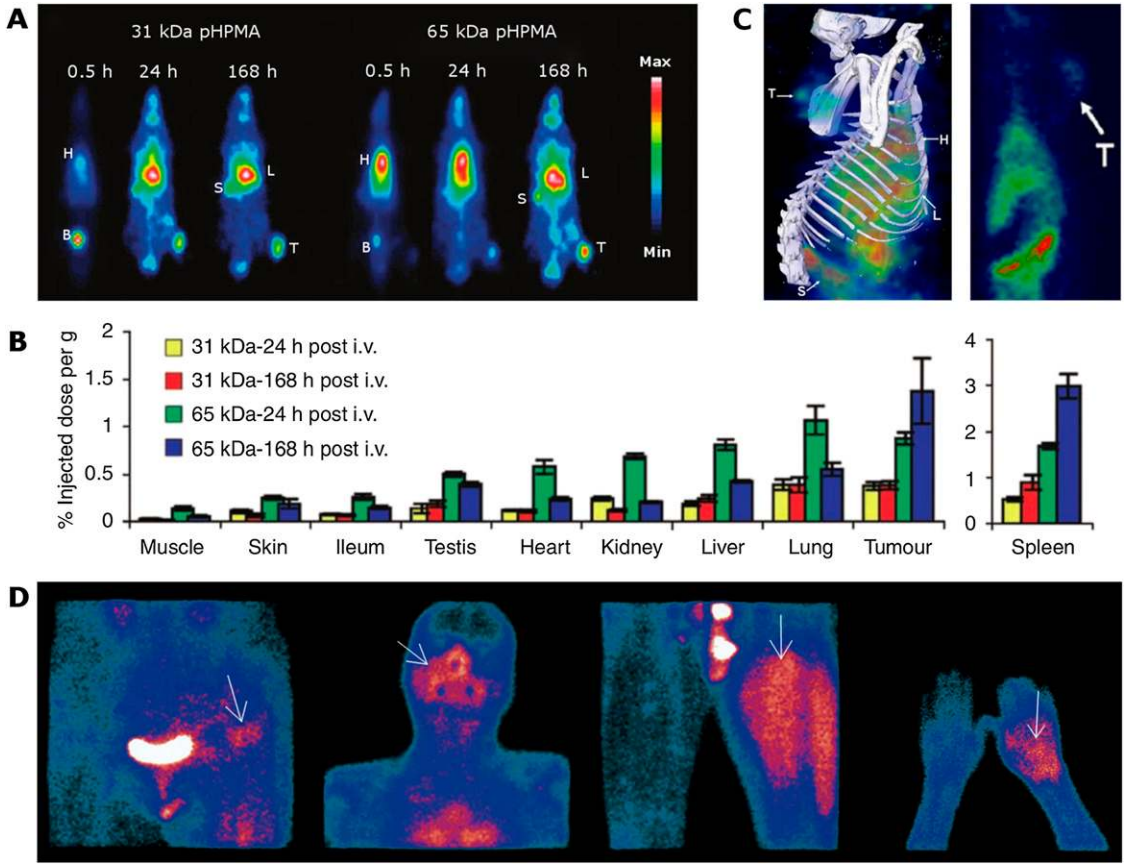

these properties have a strong impact on drug loading capacity and release, and on the stability of nanoparticles.[14,77,78]

The impact of nanoparticle size on its *in vivo* behaviour is one of the best investigated aspects of nanoparticle pharmacokinetics and biodistribution. Currently, it has been accepted that 10–100 nm is the optimal size for drug delivery systems. These nanoparticle formulations take the advantage of the EPR effect in tumours and avoid elimination in the spleen.[79,80] Furthermore, small particle size increases accumulation and enhances the penetration into tissue. Thus, nanoparticle size and surface composition are important determinants to achieve effective target site accumulation.[81] In addition, nanoparticle dispersion and variation in size play an essential role for their *in vivo* behaviour. Polydispersed nanoparticles tend to possess a range of retention times and biodistribution. Therefore, a controlled synthesis, ideally creating nanoparticles with identical properties in size, shape, charge and, in the case of functionalization, an equal amount of functional groups bound to the particle's surface, should be sought if a uniform distribution is required. Only monodispersed nanoparticles are expected to display the same biological half-life, biodistribution and target affinity *in vivo*.[73,78]

Another property of nanoparticles is their multivalency. Nanoparticles are characterized by a high surface area to volume ratio leading to a high loading capacity for diverse imaging probes, targeting ligands and therapeutic formulations. For example, a carbon nanotube with similar volume to a typical large protein (100–150 kDa) offers a 15-fold larger surface area compared with the protein.[82] This enlarged surface area allows coupling of a large amount of targeting ligands to the nanoparticle, which may significantly enhance target binding. Furthermore, nanoparticle shape is an important determinant of the *in vivo* behaviour and biological function, as it especially influences the

internalization of the nanoparticles into cells.[78,83] For example, a comparison in biodistribution between PEGylated rod-shaped gold nanoparticles and their PEGylated spherical counterparts showed that the gold nanorods were taken up to a lesser extent by the liver and macrophages and showed longer circulation times and a higher accumulation in tumour tissue compared with the spherical nanoparticles.[77] The modification of the nanoparticle surface and charge can be used to enhance or reduce their circulation time.[78,84] It has been demonstrated that polystyrene microparticles with a primary amine at the surface underwent more phagocytosis than microparticles having sulphate, hydroxyl and carboxyl groups.[81] Based on these findings, it is well accepted that positively charged nanoparticles possess a higher rate of non-specific internalization and a shorter blood circulation time compared with neutral or negatively charged nanoparticle formulations.[1,77,78,85]

Several tuning opportunities and surface modifications exist to influence the *in vivo* behaviour and to alter the biodistribution of nanoparticles. Polyethyleneglycol (PEG) is a frequently used coating material for modifying the surface of nanoparticles. PEG molecules form a protective hydrophilic layer that helps to avoid recognition by the immune system, thereby reducing the uptake of PEG-coated nanoparticles by macrophages of the MPS, a process known as stealth effect, and enhancing their circulation half-life and subsequent accumulation in target tissues. Another well known and widely used coating material is dextran.[86] For example, SPIO and USPIO nanoparticles, which are used as MRI contrast agents to image the MPS, are often coated with dextran or carboxydextran.

Besides surface modifications of nanoparticles, also nanoparticle formulations that respond to a variety of intrinsic stimuli of the tumour microenvironment, such as low pH, or over-expressed enzymes, as well as to externally applied stimuli such as ultrasound, magnetic field, hyperthermia or light, have been developed to trigger site-specific drug release.[1,6,51] For example, the utilization of temperature-sensitive liposomes containing both chemotherapeutic agents and MRI contrast agents enabled monitoring temperature-triggered drug release by examining changes in relaxation times.[87] Often trigger-responsive MR contrast agent takes the use of the chemical exchange saturation transfer (CEST) effect. These contrast media are a unique class of MR contrast agents that comprise an alternative to relaxivity-based contrast agents. CEST agents are characterized by the presence of exchangeable protons (*e.g.* -NH, -OH) being resonant at a different frequency. After selective saturation of these protons with an MR pulse, they exchange with protons of the bulk water leading to a drop in signal intensity of the water peak, which can be measured.[87–89] In a study by Langereis et al, a combined temperature-sensitive liposomal ^{1}H CEST and ^{19}F MR contrast agent was assessed as a potential carrier system for MR-guided drug delivery in combination with high-intensity focused ultrasound-induced (HIFU) hyperthermia. Both the CEST agent and the ^{19}F MR probe were co-loaded into the aqueous interior of liposomes. At temperatures below the melting point of the liposomal bilayer, the CEST effect facilitated the localization of the liposomes, while the ^{19}F signal was quenched. Upon heating, reaching temperatures above the melting point of the liposomal bilayer, the CEST agent and the ^{19}F probe were released from the aqueous interior of the liposomes, the CEST signal disappeared, and the raising ^{19}F MR signal could be used to quantify local drug release.[89] Such stimuli-sensitive nanoparticle formulations may provide real-time feedback on the efficacy of temperature-induced drug release when used in combination with local radiofrequency ablation or MR image-guided HIFU-mediated hyperthermia.[1,6,87,89]

THERANOSTICS AND THERAPY INDIVIDUALIZATION

The concept of theranostics incorporates two distinct approaches, which encompass all steps of a patient's healthcare management (Figure 4): the "biomarker" or "companion diagnostics" approach offers the opportunity to assist treatment selection, response prediction and treatment monitoring, while the "image guidance" approach allows planning, preoperative guidance and follow-up of the therapeutic action, including, for example, local drug delivery. Companion diagnostics are diagnostic clinical tests on specific biomarkers or biological targets that aim to identify patients who are (more) likely to benefit from a specific treatment by elucidating the efficacy and/or safety of a specific drug for a targeted patient group. Furthermore, companion diagnostics can provide information about the target receptor density. Companion diagnostics can be

Figure 4. Concepts for theranostics and personalized medicine. Such strategies include patient screening, diagnosis, treatment and follow-up monitoring, and are based on "companion diagnostics" and "image-guidance." The application of companion diagnostics allows patient preselection based on patient profiling of specific biomarkers or gene signatures and enables therapy selection and treatment response prediction. Image-guided drug delivery of theranostic nanoparticles enables monitoring of their biodistribution and target site accumulation, the visualization and quantification of their local activation and sometimes even drug release and the non-invasive and longitudinal assessment of their therapeutic efficacy.

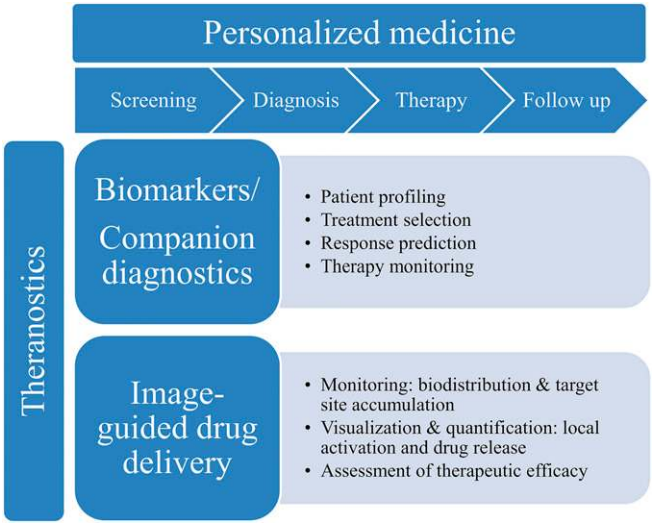

categorized into two main groups, comprising assays that have been developed after a therapeutic drug has come to the market and assays that are developed in conjunction, as companion to a specific therapeutic agent. The co-development of companion diagnostics offers the potential to significantly alter the drug development process and commercialization of potential drug candidates by yielding safer drugs with enhanced therapeutic efficacy in a faster and more cost-efficient manner. An example of a companion diagnostic imaging agent is etarfolatide (FOLCEPRI®; Endocyte Inc., West Lafayette, IN). It consists of a small-molecule high-affinity ligand for the folate receptor linked to ^{99m}Tc for SPECT imaging. Etarfolatide is used in platinum-resistant ovarian cancer or non-small-cell lung cancer to stratify patients for treatment with the folate receptor-targeted chemotherapeutic drug vintafolide (Vynfinit®; Endocyte Inc.).[90]

The combination of diagnostic and therapeutic properties into a single nano- or microparticle formulation for theranostic purposes holds significant potential for image-guided drug delivery and personalized therapies (Figure 4).[91–93] Theranostic nanoparticles enable monitoring of their biodistribution and target site accumulation, the visualization and quantification of their local activation and sometimes even drug release and the non-invasive and longitudinal assessment of their therapeutic efficacy.[11,12,91,94–96] In this context, Lammers et al[97] for instance investigated the potential of poly(n-butyl-cyanoacrylate)-based microbubbles which contained USPIO nanoparticles in their shell to simultaneously induce and monitor blood–brain barrier permeation. Transcranial ultrasound-mediated microbubble destruction led to USPIO release and the permeation of the blood–brain barrier was subsequently visualized and quantified by MRI. Such theranostic strategies are considered to be useful for monitoring and assessing efficient and safe drug delivery across biological barriers.

The application of theranostic nanoparticles may facilitate patient preselection based on non-invasive imaging, providing insights on drug delivery, drug release and drug efficacy, and predicting which patients are likely to respond to nanomedicine treatments. In addition, preselected and nanomedicine-treated patients can be longitudinally monitored to visualize their responsiveness to the administered nanomedicine formulation. Patients showing insufficient therapeutic response can be assigned to alternative therapies to facilitate and refine individualized treatment interventions.[8,11,90,98] Therefore, theranostic nanoparticles hold significant potential for enabling personalized medicine and patient individualization by optimizing treatment strategies and drug delivery and by longitudinally monitoring therapy efficacy.

CONCLUSION

Nanoparticle formulations can be applied for various purposes and can be used as cancer diagnostics and therapeutics. From a diagnostic perspective, there is significant need for a diagnostic agent capable of characterizing EPR. Theranostic nanoparticles may be applied to visualize and quantify the biodistribution and target site accumulation of nanoparticles, to monitor drug release and long-term drug efficacy and to predict a potential treatment response. Thereby, theranostic nanoparticle formulations enable preselection of patients to an optimal (nano-) chemotherapeutic formulation and seem to facilitate the concept of personalized medicine and patient individualization.

Furthermore, nanoparticles are suited to characterize tumour angiogenesis and very small nanoparticles <5 nm may also be used as molecular diagnostics for extravascular targets. However, while therapeutic nanoparticle formulations are usually designed to have slow renal excretion and long blood circulation times to improve their accumulation at the pathological site and thereby to increase therapeutic efficacy, for target-specific diagnostic nanoparticles, short blood circulation times are preferred to keep the unspecific background low and to develop a translatable clinical imaging scenario. In this context, when designing a nanoparticulate diagnostic agent, its advantage over low-molecular-weight drugs should always be carefully considered.

Finally, to further promote the clinical translation of nanoparticle formulations for diagnostic and therapeutic purposes and to further improve their implementation for personalized medicine, especially in the field of oncology, it is essential to resolve the main regulatory challenges of a controlled nanoparticle synthesis, uniformity, batch-to-batch reproducibility and upscaling of nanoparticle production. This is of utmost importance as batch-dependent differences in nanoparticle size, charge and shape possess a tremendous impact on blood circulation time, biodistribution and elimination of the nanoparticles.

Thus, to further promote the clinical translation of nanoparticles for diagnostic and therapeutic purposes and to improve the development of clinically relevant nanodiagnostics, an increased interdisciplinary collaboration and knowledge exchange between scientists from various disciplines is necessary.

FUNDING

This work was supported by the European Research Council (ERC Starting grant no. 309495: NeoNaNo).

REFERENCES

1. Bao G, Mitragotri S, Tong S. Multifunctional nanoparticles for drug delivery and molecular imaging. *Annu Rev Biomed Eng* 2013; **15**: 253–82. doi: 10.1146/annurev-bioeng-071812-152409
2. Cormode DP, Skajaa T, Fayad ZA, Mulder WJ. Nanotechnology in medical imaging: probe design and applications. *Arterioscler Thromb Vasc Biol* 2009; **29**: 992–1000. doi: 10.1161/ATVBAHA.108.165506
3. Key J, Leary JF. Nanoparticles for multimodal *in vivo* imaging in nanomedicine. *Int J Nanomedicine* 2014; **9**: 711–26. doi: 10.2147/IJN.S53717
4. Chen ZY, Wang YX, Lin Y, Zhang JS, Yang F, Zhou QL, et al. Advance of molecular imaging technology and targeted imaging agent in imaging and therapy. *Biomed Res Int* 2014; **2014**: 819324. doi: 10.1155/2014/819324

5. Weissleder R, Pittet MJ. Imaging in the era of molecular oncology. *Nature* 2008; **452**: 580–9. doi: 10.1038/nature06917
6. Kiessling F, Mertens ME, Grimm J, Lammers T. Nanoparticles for imaging: top or flop? *Radiology* 2014; **273**: 10–28. doi: 10.1148/radiol.14131520
7. Duncan R, Gaspar R. Nanomedicine(s) under the microscope. *Mol Pharm* 2011; **8**: 2101–41. doi: 10.1021/mp200394t
8. Rizzo LY, Theek B, Storm G, Kiessling F. Lammers T. Recent progress in nanomedicine: therapeutic, diagnostic and theranostic applications. *Curr Opin Biotechnol* 2013; **24**: 1159–66. doi: 10.1016/j.copbio.2013.02.020
9. Mohanraj VJ, Chen Y. Nanoparticles—a review. *Trop J Pharm Res* 2006; **5**: 561–73.
10. Lammers T, Aime S, Hennink WE, Storm G, Kiessling F. Theranostic nanomedicine. *Acc Chem Res* 2011; **44**: 1029–38. doi: 10.1021/ar200019c
11. Theek B, Rizzo LY, Ehling J, Kiessling F, Lammers T. The theranostic path to personalized nanomedicine. *Clin Transl Imaging* 2014; **2**: 66–76. doi: 10.1007/s40336-014-0051-5
12. Lammers T, Rizzo LY, Storm G, Kiessling F. Personalized nanomedicine. *Clin Cancer Res* 2012; **18**: 4889–94. doi: 10.1158/1078-0432.CCR-12-1414
13. Kim BY, Rutka JT, Chan WC. Nanomedicine. *N Eng J Med* 2010; **363**: 2434–43. doi: 10.1056/NEJMra0912273
14. Sumer B, Gao J. Theranostic nanomedicine for cancer. *Nanomedicine (Lond)* 2008; **3**: 137–40. doi: 10.2217/17435889.3.2.137
15. Chen X, Gambhir SS, Cheon J. Theranostic nanomedicine. *Acc Chem Res* 2011; **44**: 841. doi: 10.1021/ar200231d
16. Kunjachan S, Jayapaul J, Mertens ME, Storm G, Kiessling F, Lammers T. Theranostic systems and strategies for monitoring nanomedicine-mediated drug targeting. *Curr Pharm Biotechnol* 2012; **13**: 609–22. doi: 10.2174/138920112799436302
17. Ehling J, Lammers T, Kiessling F. Non-invasive imaging for studying anti-angiogenic therapy effects. *Thromb Haemost* 2013; **109**: 375–90. doi: 10.1160/TH12-10-0721
18. Lanza GM, Caruthers SD, Winter PM, Hughes MS, Schmieder AH, Hu G, et al. Angiogenesis imaging with vascular-constrained particles: the why and how. *Eur J Nucl Med Mol Imaging* 2010; **37**(Suppl. 1): S114–26. doi: 10.1007/s00259-010-1502-5
19. Geninatti Crich S, Bussolati B, Tei L, Grange C, Esposito G, Lanzardo S, et al. Magnetic resonance visualization of tumor angiogenesis by targeting neural cell adhesion molecules with the highly sensitive gadolinium-loaded apoferritin probe. *Cancer Res* 2006; **66**: 9196–201. doi: 10.1158/0008-5472.CAN-06-1728
20. Zhang C, Jugold M, Woenne EC, Lammers T, Morgenstern B, Mueller MM, et al. Specific targeting of tumor angiogenesis by RGD-conjugated ultrasmall superparamagnetic iron oxide particles using a clinical 1.5-T magnetic resonance scanner. *Cancer Res* 2007; **67**: 1555–62. doi: 10.1158/0008-5472.CAN-06-1668
21. Preda A, van Vliet M, Krestin GP, Brasch RC, van Dijke CF. Magnetic resonance macromolecular agents for monitoring tumor microvessels and angiogenesis inhibition. *Invest Radiol* 2006; **41**: 325–31. doi: 10.1097/01.rli.0000186565.21375.88
22. Kiessling F, Morgenstern B, Zhang C. Contrast agents and applications to assess tumor angiogenesis *in vivo* by magnetic resonance imaging. *Curr Med Chem* 2007; **14**: 77–91. doi: 10.2174/092986707779313516
23. Winter PM, Cai K, Chen J, Adair CR, Kiefer GE, Athey PS, et al. Targeted PARACEST nanoparticle contrast agent for the detection of fibrin. *Magn Reson Med* 2006; **56**: 1384–8. doi: 10.1002/mrm.21093
24. Cassidy MC, Chan HR, Ross BD, Bhattacharya PK, Marcus CM. *In vivo* magnetic resonance imaging of hyperpolarized silicon particles. *Nat Nanotechnol* 2013; **8**: 363–8. doi: 10.1038/nnano.2013.65
25. Leike J, Sachse A, Ehritt C, Krause W. Biodistribution and CT-imaging characteristics of iopromide-carrying liposomes in rats. *J Liposome Res* 1996; **6**: 665–80. doi: 10.3109/08982109609039920
26. Torchilin VP, Frank-Kamenetsky MD, Wolf GL. CT visualization of blood pool in rats by using long-circulating, iodine-containing micelles. *Acad Radiol* 1999; **6**: 61–5. doi: 10.1016/S1076-6332(99)80063-4
27. Liu Y, Ai K, Liu J, Yuan Q, He Y, Lu L. Hybrid BaYbF(5) nanoparticles: novel binary contrast agent for high-resolution *in vivo* X-ray computed tomography angiography. *Adv Healthc Mater* 2012; **1**: 461–6. doi: 10.1002/adhm.201200028
28. Jakhmola A, Anton N, Vandamme TF. Inorganic nanoparticle based contrast agents for X-ray computed tomography. *Adv Healthc Mater* 2012; **1**: 413–31. doi: 10.1002/adhm.201200032
29. Kim YH, Jeon J, Hong SH, Rhim WK, Lee YS, Youn H, et al. Tumor targeting and imaging using cyclic RGD-PEGylated gold nanoparticle probes with directly conjugated iodine-125. *Small* 2011; **7**: 2052–60. doi: 10.1002/smll.201100927
30. Rabin O, Manuel Perez J, Grimm J, Wojtkiewicz G, Weissleder R. An X-ray computed tomography imaging agent based on long-circulating bismuth sulphide nanoparticles. *Nat Mater* 2006; **5**: 118–22. doi: 10.1038/nmat1571
31. Bzyl J, Lederle W, Rix A, Grouls C, Tardy I, Pochon S, et al. Molecular and functional ultrasound imaging in differently aggressive breast cancer xenografts using two novel ultrasound contrast agents (BR55 and BR38). *Eur Radiol* 2011; **21**: 1988–95. doi: 10.1007/s00330-011-2138-y
32. Kiessling F, Bzyl J, Fokong S, Siepmann M, Schmitz G, Palmowski M. Targeted ultrasound imaging of cancer: an emerging technology on its way to clinics. *Curr Pharm Des* 2012; **18**: 2184–99. doi: 10.2174/138161212800099900
33. Pysz MA, Foygel K, Rosenberg J, Gambhir SS, Schneider M, Willmann JK. Antiangiogenic cancer therapy: monitoring with molecular US and a clinically translatable contrast agent (BR55). *Radiology* 2010; **256**: 519–27. doi: 10.1148/radiol.10091858
34. Gao Z, Kennedy AM, Christensen DA, Rapoport NY. Drug-loaded nano/microbubbles for combining ultrasonography and targeted chemotherapy. *Ultrasonics* 2008; **48**: 260–70. doi: 10.1016/j.ultras.2007.11.002
35. Kang E, Min HS, Lee J, Han MH, Ahn HJ, Yoon IC, et al. Nanobubbles from gas-generating polymeric nanoparticles: ultrasound imaging of living subjects. *Angew Chem Int Ed Engl* 2010; **49**: 524–8. doi: 10.1002/anie.200903841
36. Kim K, Kim JH, Park H, Kim YS, Park K, Nam H, et al. Tumor-homing multifunctional nanoparticles for cancer theragnosis: simultaneous diagnosis, drug delivery, and therapeutic monitoring. *J Control Release* 2010; **146**: 219–27. doi: 10.1016/j.jconrel.2010.04.004
37. Gao X, Cui Y, Levenson RM, Chung LW, Nie S. *In vivo* cancer targeting and imaging with semiconductor quantum dots. *Nat Biotechnol* 2004; **8**: 969–76.
38. Santra S, Dutta D, Walter GA, Moudgil BM. Fluorescent nanoparticle probes for cancer imaging. *Technol Cancer Res Treat* 2005; **4**: 593–602. doi: 10.1177/153303460500400603
39. Cai X, Li W, Kim CH, Yuan Y, Wang LV, Xia Y. *In vivo* quantitative evaluation of the transport kinetics of gold nanocages in a lymphatic system by noninvasive photoacoustic tomography. *ACS Nano* 2011; **5**: 9658–67. doi: 10.1021/nn203124x
40. De la Zerda A, Zavaleta C, Keren S, Vaithilingam S, Bodapati S, Liu Z, et al. Carbon nanotubes as photoacoustic molecular imaging agents in living mice. *Nat*

Nanotechnol 2008; **3**: 557–62. doi: 10.1038/nnano.2008.231
41. Akers WJ, Kim C, Berezin M, Guo K, Fuhrhop R, Lanza GM, et al. Noninvasive photoacoustic and fluorescence sentinel lymph node identification using dye-loaded perfluorocarbon nanoparticles. *ACS Nano* 2011; **5**: 173–82. doi: 10.1021/nn102274q
42. Xie H, Wang ZJ, Bao A, Goins B, Phillips WT. *In vivo* PET imaging and biodistribution of radiolabeled gold nanoshells in rats with tumor xenografts. *Int J Pharm* 2010; **395**: 324–30. doi: 10.1016/j.ijpharm.2010.06.005
43. Majmudar MD, Yoo J, Keliher EJ, Truelove JJ, Iwamoto Y, Sena B, et al. Polymeric nanoparticle PET/MR imaging allows macrophage detection in atherosclerotic plaques. *Circ Res* 2013; **112**: 755–61. doi: 10.1161/CIRCRESAHA.111.300576
44. Ocampo-García BE, Ramírez Fde M, Ferro-Flores G, De León-Rodríguez LM, Santos-Cuevas CL, Morales-Avila E, et al. (99m)Tc-labelled gold nanoparticles capped with HYNIC-peptide/mannose for sentinel lymph node detection. *Nucl Med Biol* 2011; **38**: 1–11. doi: 10.1016/j.nucmedbio.2010.07.007
45. Koukourakis MI, Koukouraki S, Giatromanolaki A, Kakolyris S, Georgoulias V, Velidaki A, et al. High intratumoral accumulation of stealth liposomal doxorubicin in sarcomas—rationale for combination with radiotherapy. *Acta Oncol* 2000; **39**: 207–11. doi: 10.1080/028418600430789
46. Brouwer OR, Buckle T, Vermeeren L, Klop WM, Balm AJ, van der Poel HG, et al. Comparing the hybrid fluorescent-radioactive tracer indocyanine green-99mTc-nanocolloid with 99mTc-nanocolloid for sentinel node identification: a validation study using lymphoscintigraphy and SPECT/CT. *J Nucl Med* 2012; **53**: 1034–40. doi: 10.2967/jnumed.112.103127
47. Rubin GD. Computed tomography: revolutionizing the practice of medicine for 40 years. *Radiology* 2014; **273**(Suppl. 2): S45–74. doi: 10.1148/radiol.14141356
48. Strijkers GJ, Mulder WJ, van Tilborg GA, Nicolay K. MRI contrast agents: current status and future perspectives. *Anticancer Agents Med Chem* 2007; **7**: 291–305. doi: 10.2174/187152007780618135
49. Nyström AM, Fadeel B. Safety assessment of nanomaterials: implications for nanomedicine. *J Control Release* 2012; **161**: 403–8. doi: 10.1016/j.jconrel.2012.01.027
50. Kircher MF, de la Zerda A, Jokerst JV, Zavaleta CL, Kempen PJ, Mittra E, et al. A brain tumor molecular imaging strategy using a new triple-modality MRI-photoacoustic-Raman nanoparticle. *Nat Med* 2012; **18**: 829–34. doi: 10.1038/nm.2721
51. Kaittanis C, Shaffer TM, Ogirala A, Santra S, Perez JM, Chiosis G, et al. Environment-responsive nanophores for therapy and treatment monitoring *via* molecular MRI quenching. *Nat Commun* 2014; **5**: 3384. doi: 10.1038/ncomms4384
52. Allen TM, Cullis PR. Liposomal drug delivery systems: from concept to clinical applications. *Adv Drug Deliv Rev* 2013; **65**: 36–48. doi: 10.1016/j.addr.2012.09.037
53. Seymour LW, Ferry DR, Kerr DJ, Rea D, Whitlock M, Poyner R, et al. Phase II studies of polymer-doxorubicin (PK1, FCE28068) in the treatment of breast, lung and colorectal cancer. *Int J Oncol* 2009; **34**: 1629–36. doi: 10.3892/ijo_00000293
54. Phillips E, Penate-Medina O, Zanzonico PB, Carvajal RD, Mohan P, Ye Y, et al. Clinical translation of an ultrasmall inorganic optical-PET imaging nanoparticle probe. *Sci Transl Med* 2014; **6**: 260ra149. doi: 10.1126/scitranslmed.3009524
55. Bashir MR, Bhatti L, Marin D, Nelson RC. Emerging applications for ferumoxytol as a contrast agent in MRI. *J Magn Reson Imaging* 2015; **41**: 884–98. doi: 10.1002/jmri.24691
56. Desser TS, Rubin DL, Muller H, McIntire GL, Bacon ER, Toner JL. Blood pool and liver enhancement in CT with liposomal iodixanol: comparison with iohexol. *Acad Radiol* 1999; **6**: 176–83. doi: 10.1016/S1076-6332(99)80404-8
57. Schmitz SA, Taupitz M, Wagner S, Wolf KJ, Beyersdorff D, Hamm B. Magnetic resonance imaging of artherosclerotic plaques using superparamagnetic iron oxide particles. *J Magn Reson Imaging* 2001; **14**: 355–61. doi: 10.1002/jmri.1194
58. Sever AR, Mills P, Weeks J, Jones SE, Fish D, Jones PA, et al. Preoperative needle biopsy of sentinel lymph nodes using intradermal microbubbles and contrast-enhanced ultrasound in patients with breast cancer. *AJR Am J Roentgenol* 2012; **199**: 465–70. doi: 10.2214/AJR.11.7702
59. Kim S, Lim YT, Soltesz EG, De Grand AM, Lee J, Nakayama A, et al. Near-infrared fluorescent type II quantum dots for sentinel lymph node mapping. *Nat Biotechnol* 2004; **22**: 93–7. doi: 10.1038/nbt920
60. Weissleder R, Elizondo G, Stark DD, Hahn PF, Marfil J, Gonzalez JF, et al. The diagnosis of splenic lymphoma by MR imaging: value of superparamagnetic iron oxide. *AJR Am J Roentgenol* 1989; **152**: 175–80. doi: 10.2214/ajr.152.1.175
61. Rappeport ED, Loft A, Berthelsen AK, von der Recke P, Larsen PN, Mogensen AM, et al. Contrast-enhanced FDG-PET/CT *vs.* SPIO-enhanced MRI *vs.* FDG-PET *vs.* CT in patients with liver metastases from colorectal cancer: a prospective study with intraoperative confirmation. *Acta Radiol* 2007; **48**: 369–78. doi: 10.1080/02841850701294560
62. Harisinghani MG, Barentsz J, Hahn PF, Deserno WM, Tabatabaei S, van de Kaa CH, et al. Noninvasive detection of clinically occult lymph-node metastases in prostate cancer. *N Engl J Med* 2003; **348**: 2491–9. doi: 10.1056/NEJMoa022749
63. Palmowski M, Huppert J, Ladewig G, Hauff P, Reinhardt M, Mueller MM, et al. Molecular profiling of angiogenesis with targeted ultrasound imaging: early assessment of antiangiogenic therapy effects. *Mol Cancer Ther* 2008; **7**: 101–9. doi: 10.1158/1535-7163.MCT-07-0409
64. Mulder WJ, Strijkers GJ, Habets JW, Bleeker EJ, van der Schaft DW, Storm G, et al. MR molecular imaging and fluorescence microscopy for identification of activated tumor endothelium using a bimodal lipidic nanoparticle. *FASEB J* 2005; **19**: 2008–10.
65. Kunjachan S, Pola R, Gremse F, Theek B, Ehling J, Moeckel D, et al. Passive *versus* active tumor targeting using RGD- and NGR-modified polymeric nanomedicines. *Nano Lett* 2014; **14**: 972–81. doi: 10.1021/nl404391r
66. Mulder WJ, van der Schaft DW, Hautvast PA, Strijkers GJ, Koning GA, Storm G, et al. Early *in vivo* assessment of angiostatic therapy efficacy by molecular MRI. *FASEB J* 2007; **21**: 378–83. doi: 10.1096/fj.06-6791com
67. Matsumura Y, Maeda H. A new concept for macromolecular therapeutics in cancer chemotherapy: mechanism of tumoritropic accumulation of proteins and the antitumor agent smancs. *Cancer Res* 1986; **46**: 6387–92.
68. Maeda H, Wu J, Sawa T, Matsumura Y, Hori K. Tumor vascular permeability and the EPR effect in macromolecular therapeutics: a review. *J Control Release* 2000; **65**: 271–84. doi: 10.1016/S0168-3659(99)00248-5
69. Torchilin V. Tumor delivery of macromolecular drugs based on the EPR effect. *Adv Drug Deliv Rev* 2011; **63**: 131–5. doi: 10.1016/j.addr.2010.03.011
70. Nehoff H, Parayath NN, Domanovitch L, Taurin S, Greish K. Nanomedicine for drug targeting: strategies beyond the enhanced permeability and retention effect. *Int J Nanomedicine* 2014; **9**: 2539–55. doi: 10.2147/IJN.S47129
71. Jain RK, Stylianopoulos T. Delivering nanomedicine to solid tumors. *Nat Rev Clin Oncol* 2010; **7**: 653–64. doi: 10.1038/nrclinonc.2010.139
72. Prabhakar U, Maeda H, Jain RK, Sevick-Muraca EM, Zamboni W, Farokhzad OC,

et al. Challenges and key considerations of the enhanced permeability and retention effect for nanomedicine drug delivery in oncology. *Cancer Res* 2013; **73**: 2412–17. doi: 10.1158/0008-5472.CAN-12-4561
73. Svenson S. Theranostics: are we there yet? *Mol Pharm* 2013; **10**: 848–56. doi: 10.1021/mp300644n
74. Lammers T, Subr V, Peschke P, Kühnlein R, Hennink WE, Ulbrich K, et al. Image-guided and passively tumour-targeted polymeric nanomedicines for radiochemotherapy. *Br J Cancer* 2008; **99**: 900–10. doi: 10.1038/sj.bjc.6604561
75. Soundararajan A, Bao A, Phillips WT, Perez R 3rd, Goins BA. [(186)Re]Liposomal doxorubicin (Doxil): *in vitro* stability, pharmacokinetics, imaging and biodistribution in a head and neck squamous cell carcinoma xenograft model. *Nucl Med Biol* 2009; **36**: 515–24. doi: 10.1016/j.nucmedbio.2009.02.004
76. Soundararajan A, Dodd GD 3rd, Bao A, Phillips WT, McManus LM, Prihoda TJ, et al. Chemo-radionuclide therapy with 186Re-labeled liposomal doxorubicin in combination with radiofrequency ablation for effective treatment of head and neck cancer in a nude rat tumor xenograft model. *Radiology* 2011; **261**: 813–23. doi: 10.1148/radiol.11110361
77. Longmire MR, Ogawa M, Choyke PL, Kobayashi H. Biologically optimized nano-sized molecules and particles: more than just size. *Bioconjug Chem* 2011; **22**: 993–1000. doi: 10.1021/bc200111p
78. Grimm J, Scheinberg DA. Will nanotechnology influence targeted cancer therapy? *Semin Radiat Oncol* 2011; **21**: 80–7. doi: 10.1016/j.semradonc.2010.10.003
79. Aslan B, Ozpolat B, Sood AK, Lopez-Berestein G. Nanotechnology in cancer therapy. *J Drug Target* 2013; **21**: 904–13. doi: 10.3109/1061186X.2013.837469
80. Petros RA, DeSimone JM. Strategies in the design of nanoparticles for therapeutic applications. *Nat Rev Drug Discov* 2010; **9**: 615–27. doi: 10.1038/nrd2591
81. Alexis F, Pridgen E, Molnar LK, Farokhzad OC. Factors affecting the clearance and biodistribution of polymeric nanoparticles. *Mol Pharm* 2008; **5**: 505–15. doi: 10.1021/mp800051m
82. Scheinberg DA, Villa CH, Escorcia FE, McDevitt MR. Conscripts of the infinite armada: systemic cancer therapy using nanomaterials. *Nat Rev Clin Oncol* 2010; **7**: 266–76. doi: 10.1038/nrclinonc.2010.38
83. Gratton SE, Ropp PA, Pohlhaus PD, Luft JC, Madden VJ, Napier ME, et al. The effect of particle design on cellular internalization pathways. *Proc Natl Acad Sci U S A* 2008; **105**: 11613–18. doi: 10.1073/pnas.0801763105
84. Kaittanis C, Shaffer TM, Thorek DL, Grimm J. Dawn of advanced molecular medicine: nanotechnological advancements in cancer imaging and therapy. *Crit Rev Oncog* 2014; **19**: 143–76. doi: 10.1615/CritRevOncog.2014011601
85. Longmire M, Choyke PL, Kobayashi H. Clearance properties of nano-sized particles and molecules as imaging agents: considerations and caveats. *Nanomedicine (Lond)* 2008; **3**: 703–17. doi: 10.2217/17435889.3.5.703
86. Moore A, Marecos E, Bogdanov A Jr, Weissleder R. Tumoral distribution of long-circulating dextran-coated iron oxide nanoparticles in a rodent model. *Radiology* 2000; **214**: 568–74. doi: 10.1148/radiology.214.2.r00fe19568
87. Grüll H, Langereis S. Hyperthermia-triggered drug delivery from temperature-sensitive liposomes using MRI-guided high intensity focused ultrasound. *J Control Release* 2012; **161**: 317–27. doi: 10.1016/j.jconrel.2012.04.041
88. Castelli DD, Terreno E, Longo D, Aime S. Nanoparticle-based chemical exchange saturation transfer (CEST) agents. *NMR Biomed* 2013; **26**: 839–49. doi: 10.1002/nbm.2974
89. Langereis S, Keupp J, van Velthoven JL, de Roos IH, Burdinski D, Pikkemaat JA, et al. A temperature-sensitive liposomal 1H CEST and 19F contrast agent for MR image-guided drug delivery. *J Am Chem Soc* 2009; **131**: 1380–1. doi: 10.1021/ja8087532
90. Maurer AH, Elsinga P, Fanti S, Nguyen B, Oyen WJ, Weber WA. Imaging the folate receptor on cancer cells with 99mTc-etarfolatide: properties, clinical use, and future potential of folate receptor imaging. *J Nucl Med* 2014; **55**: 701–4. doi: 10.2967/jnumed.113.133074
91. Lammers T, Kiessling F, Hennink WE, Storm G. Nanotheranostics and image-guided drug delivery: current concepts and future directions. *Mol Pharm* 2010; **7**: 1899–912. doi: 10.1021/mp100228v
92. Mura S, Couvreur P. Nanotheranostics for personalized medicine. *Adv Drug Deliv Rev* 2012; **64**: 1394–416. doi: 10.1016/j.addr.2012.06.006
93. Kim TH, Lee S, Chen X. Nanotheranostics for personalized nanomedicine. *Expert Rev Mol Diagn* 2013; **13**: 257–69. doi: 10.1586/erm.13.15
94. Janib SM, Moses AS, MacKay JA. Imaging and drug delivery using theranostic nanoparticles. *Adv Drug Deliv Rev* 2010; **62**: 1052–63. doi: 10.1016/j.addr.2010.08.004
95. Zhang XQ, Xu X, Bertrand N, Pridgen E, Swami A, Farokhzad OC. Interactions of nanomaterials and biological systems: implications to personalized nanomedicine. *Adv Drug Deliv Rev* 2012; **64**: 1363–84. doi: 10.1016/j.addr.2012.08.005
96. Xie J, Lee S, Chen X. Nanoparticle-based theranostic agents. *Adv Drug Deliv Rev* 2010; **62**: 1064–79. doi: 10.1016/j.addr.2010.07.009
97. Lammers T, Koczera P, Fokong S, Gremse F, Ehling J, Vogt M, et al. Theranostic USPIO-loaded microbubbles for mediating and monitoring blood-brain barrier permeation. *Adv Funct Mater* 2015; **25**: 36–43. doi: 10.1002/adfm.201401199
98. Lammers T. Smart drug delivery systems: back to the future *vs.* clinical reality. *Int J Pharm* 2013; **454**: 527–9. doi: 10.1016/j.ijpharm.2013.02.046